Published in Chemical Engineering Journal Volume 291, 1 May 2016, Pages 47–54

Structured carbon supports for the immobilization of an Rh diamine complex catalyst

C.C. Gheorghiu[a], E. García-Bordejé[b], N. Job[c], M.C. Román-Martínez[a]

[a]Department of Inorganic Chemistry and Materials Institute. University of Alicante. Carretera de San Vicente s/n. 03690 Alicante. Spain

1. Introduction

Carbon materials are recognized as suitable supports in heterogeneous catalysis due to specific characteristics such as the broad variety of morphological, textural and chemical properties, which can be modified up to certain limits, resistance to acidic/basic media, and the potential easy recovery of precious metals by support burn out [1][2].

Besides, the following properties are usually required: (i) high purity, avoiding either catalyst poisoning or the promotion of unwanted side reactions, (ii) large volumes of meso/macropores to avoid diffusion limitations, and (iii) potential specific metal-support interactions that can have positive effects on the catalytic activity and selectivity. Amongst the many carbon supports available, carbon nanofilaments (carbon nanotubes and carbon nanofibres) [3] and carbon xerogels [4][5][6] fulfill the mentioned requirements.

Carbon nanofilaments suffer, however, from technical drawbacks related with their powdery condition, which makes handling in catalytic processes troublesome. In particular, powder CNFs exhibit problems of agglomeration and difficulty of filtration in slurry phase operation, and pressure drop in gas phase operation. These inconveniences can be avoided by the incorporation of carbon filaments into larger objects like, for example, ceramic monoliths. The preparation of a ceramic monolith completely covered with a well-attached layer of carbon nanofibres (CNF) of uniform thickness has been previously reported [7][8]. Since then, CNF/monoliths have been

used as catalyst support for several gas and liquid phase reactions. In gas phase reactions, the main advantage of using CNF/monoliths is its robustness, portability and low pressure drop. Besides, immobilization of CNFs avoids their release to the atmosphere with the associated risk for human health. Ru nanoparticles have been dispersed in monoliths coated with either CNFs or N-CNFs and used in NH_3 decomposition for in-situ H_2 generation [9]. The activity of those catalysts was significantly higher than that of similar ones prepared on other supports. A Fe/CNT/monolith was demonstrated to be active for CO_2 conversion to hydrocarbons under high pressure conditions [10] while Pt and Pd on CNF/monolith have been used in the catalytic combustion of BTX (benzene, toluene and xylene) at low temperatures (< 200 ºC) [11]. The catalyst supported on CNF/monolith outperformed those supported on γ-Al_2O_3 because the hydrophobic nature of CNF favors the release of water formed during the reaction.

In reactions carried out in liquid media, the main advantages of using CNF/monolith compared to CNF slurries or bulky carbon pellets are that the difficult filtration of the CNF slurry can be avoided, and that diffusion of the reactants is faster due to the large mesopore volume and low tortuosity of CNFs, and to the short diffusional path of the catalytic layer. For example, Pd supported on CNF/TiO_2/monolith has been used for the selective hydrogenation of cinnamaldehyde (CAL)[12] obtaining a very high selectivity to HCAL (about 90%) at 95% CAL conversion. This performance is similar to that of powdered Pd/CNF (about 93%) but much better than that of Pd on activated carbon (about 45%) and Pd on mesoporous carbon (82%). Other liquid phase applications in which CNF/monoliths have shown outstanding properties are the immobilization of enzymes (lipase) for biocatalysis [13], as noble metal nanoparticle support for the reduction of nitrates and bromates in water [14][15] and as metal-free catalysts for the ozonation of organic pollutants in water [16].

In carbon xerogels, the size and volume of meso/macropores can be controlled by the synthesis procedures [17] [18], including the synthesis variables (like pH of the starting solution) and the conditions of the drying and pyrolysis of precursor gels. Regarding this last point, the evaporative drying technique was found to be the easiest and less expensive method for the synthesis of a porous carbon with a tailored texture, allowing all pore sizes to be obtained, but with the pore volume and the pores size strongly

correlated. Carbon xerogels have been used to support both, metal complexes [19], [6], [5] and metal nanoparticles [20] and the effect of the pore texture on mass transport was evidenced in gas phase catalysis [4] and in electrocatalysis [21].

As indicated above, both a CNF-monolith sample and a carbon xerogel with a proper mesoporous structure can be suitable supports of catalysts to be used in gas-liquid reactions, even more if the active phase is a relatively bulky molecular species. Because of that, in this work these two carbon materials have been used to immobilize an Rh diamine complex with the objective of preparing hybrid catalysts, combining the advantageous properties of homogeneous and heterogeneous catalysts, to be used in hydrogenation reactions. The diamine Rh complex (schematically depicted in Figure 1) is $[Rh(COD)NH_2(CH_2)_2NH(CH_2)_3Si(OCH_3)_3]BF_4$, abbreviated as Rh(NN)Si. It contains the ligand cyclooctadiene (COD) and a bidentate amine ligand with a trimethoxysilane functionality ($-Si(OCH_3)_3$). The anchoring on the support is expected to occur through a covalent siloxane-type bond created by reaction of methoxy functionalities with surface –OH type groups. In this way, the study previously carried out dealing with the immobilization of the mentioned Rh complex on different carbon materials [22] is extended to these two structured carbon-based supports.

Thus, the purpose of this work is to study the capability of a CNF-monolith sample and a granular carbon xerogel as supports in the preparation of hybrid catalyst. Using these supports allows taking advantage of both their open porous structure, which should decrease mass transfer limitations, and their morphology, which will facilitate the catalyst handling and will enable to avoid the difficult separation processes.

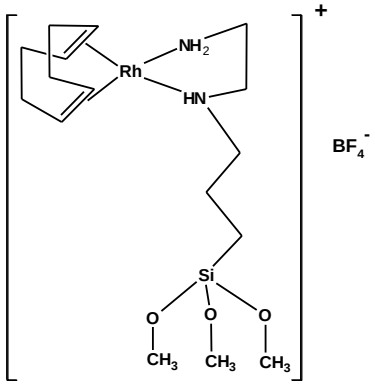

Figure 1. Chemical structure of the Rh(NN)Si complex.

2. Experimental

2.1.Supports

CNF coated monolith

The procedure used to prepare this support is as follows [23]: a cordierite monolith (from Corning, 1 cm diameter, 5 cm length, 400 cpsi (channels per squared inch)) was washcoated with alumina by dipcoating in a sol prepared with pseudoboehmite (AlOOH), urea and 0.3 M nitric acid with a weight ratio of 2:1:5. The liquid inside the monolith channels was removed by flushing pressurized air. Afterwards, the sample was dried at room temperature for 24 h while it was rotated around the longitudinal axis; then it was calcined in air at 873 K for 2 h. Nickel was deposited on the alumina washcoat as follows: the monolith sample was kept overnight in 1 L aqueous solution containing 29 g $Ni(NO_3)_2{\cdot}6H_2O$, 80 g NH_4NO_3 and 4 mL ammonia solution (25% w/w). This solution was flowing continuously through the channels. Then, the monolith was rinsed thoroughly with deionised water, dried (room temperature overnight, and 373 K for 1 h), and calcined in flowing nitrogen at 873 K for 2 h. The Ni content in the monoliths was 0.9 wt%. After reduction (hydrogen atmosphere, 873 K, 2 h), the CNF were grown by putting the sample in contact with a 100 mL/min flow of a 1:1 mixture C_2H_6:H_2 at 873 K for 3.5 h. The amount of CNF deposited corresponds to 15.5 wt% carbon and supposes an average layer thickness of about 10 µm. The CNF grown on the monolith display a BET surface area of 150 m^2/g, a micropore volume of 0.01 cm^3/g and a mesopore volume equal to 0.30 cm^3/g [24]. The sample is named M-CNF hereafter.

To prepare the catalyst, sample M-CNF was cut into several pieces of about 7 mm length that contained between 20 and 30 mg of carbon. The cutting was done very carefully with a metallic saw in order to avoid any fracture of the ceramic material.

Figure 2 shows a picture of the original M-CNF sample and of several cut pieces.

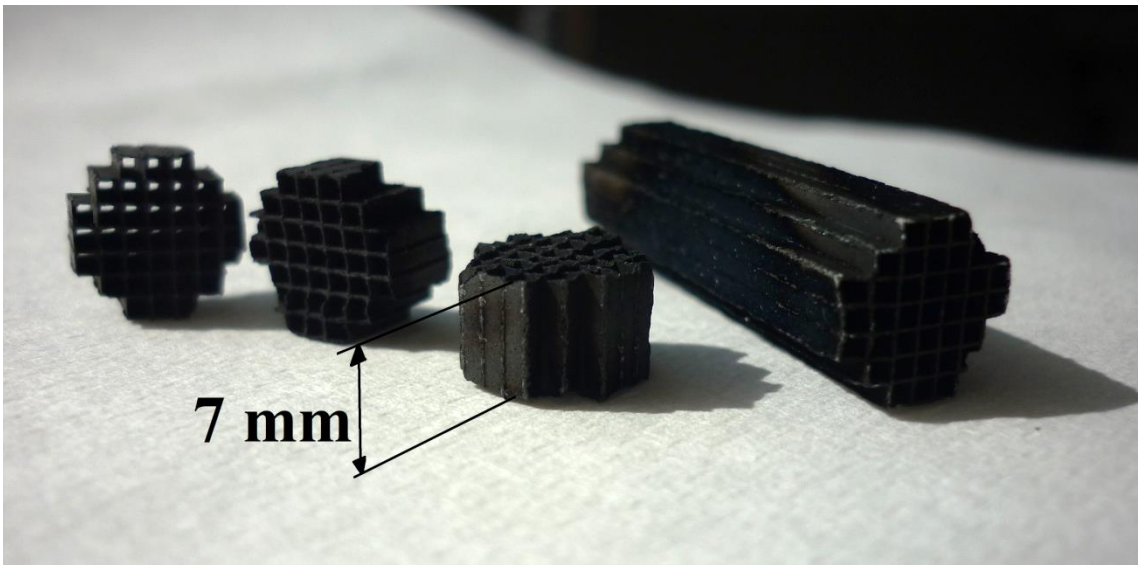

Figure 2. Pictures of the CNF-coated monolith sample (M-CNF): original form and cut pieces.

Carbon xerogel

The carbon xerogel was prepared according to a reported procedure [18], which can be summarized as follows: the carbon gel was obtained by the polycondensation of resorcinol (R) and formaldehyde (F) in deionized water (R/F molar ratio= 0.5, dilution ratio D = 5.7), using a basic agent (Na_2CO_3, denoted C) to increase the pH of the solution. The R/C molar ratio was chosen equal to 750. Gelation was performed at 85 °C for 72 h. Then, the sample was vacuum-dried at 333 K and heat treated (423 K, 0.01 bar, 12 h) in order to obtain the organic xerogel. Finally, it was pyrolyzed under nitrogen flow (1073 K, 3 h), allowing the carbon xerogel material to be obtained.

Previous to its use, the sample was grinded and sieved to ensure a particle size between 1.0 and 1.4 mm (Figure 3). The sample is named CX3.

(a) (b)

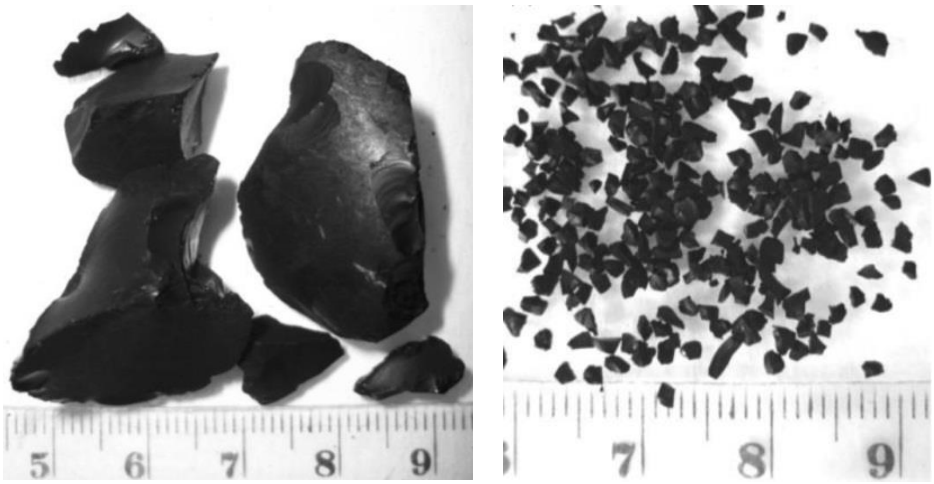

Figure 3. Pictures of the carbon xerogel CX3 sample: (a) original form and (b) grinded (1.0-1.4 mm).

Oxidation treatment

In order to develop surface oxygen complexes on both carbon supports, necessary to graft the Rh complex, they were submitted to an oxidation treatment under the following conditions: heating up to 623 K (15 K/min) was done in He and then, the gas flow was changed to synthetic air (60 mL/min) with a soak time of 3.5 h. Afterwards, the samples were cooled down in air and stored until use. The oxidized samples are named M-CNFOx and CX3Ox, respectively.

Characterization

The surface chemistry of the oxidized supports was characterized by TPD (temperature programmed desorption), using a thermobalance SDT TA Instruments 2960 coupled to a mass spectrometer Balzers MSC 200Thermostar. Approximately, 10 mg of carbon material (obtained by scrapping in the case of the M-CNF sample) were heated at 20 K/min up to 1300 K in a He flow of 20 mL/min.

The textural properties of the supports were analyzed by N_2 adsorption at 77 K, using a Micromeritics ASAP 2020 device in the case of sample M-CNFOx and an automatic volumetric apparatus Autosorb-6B (Quantachrome) in the case of support CX3Ox. The samples were previously outgassed at 523 K for 4 h. BET surface area (S_{BET}) and pore volumes of different size range (micropores, V_{μ}, and mesopores, V_{meso}) were determined as described in the literature [25]. It was checked by mercury porosimetry that the carbon materials do not contain macropores. The skeletal density (ρ_s) of the carbon structures, i.e. all open pores excluded, was measured by helium pycnometry

using a Micromeritics Accupyc 1330 device. The bulk density was calculated from the previous data as:

$$\rho_{\text{bulk}} = \frac{1}{V_{\text{v}} + \frac{1}{\rho_s}} \quad (1)$$

where V_V is the total pore volume, i.e. the sum of mesopore and micropore volumes, V_{meso} and V_μ. The void fraction corresponding to mesopores in the carbon material can be calculated as:

$$\varepsilon = \frac{V_{\text{meso}}}{V_{\text{meso}} + V_\mu + \frac{1}{\rho_s}} \quad (2)$$

The supports were also characterized by transmission and scanning electron microscopy (TEM and SEM) using the JEOL JEM-2010 and HITACHI S-3000N microscopes, respectively.

2.2.Catalysts

The synthesis of the complex $[Rh(COD)NH_2(CH_2)_2NH(CH_2)_3Si(OCH_3)_3]BF_4$, (Rh(NN)Si) was carried out using standard Schlenk techniques and following the reported procedure [26].

The synthesized Rh complex was characterized by infrared spectroscopy (FT-IR), X-ray photoelectron spectroscopy (XPS) and elemental analysis (EA), and the obtained results, which were reported elsewhere [22], indicate that the desired complex was obtained.

The hybrid catalysts were prepared by impregnation of the supports (previously outgassed at 373 K, 3 h) with a methanol solution of the Rh(NN)Si complex (5 mL solution per gram of support). The mixture was maintained under reflux for 21 h; then, the solid was removed from the solution and washed with methanol in Soxhlet for 24 h. Afterwards, the catalysts were vacuum-dried (0.01 Pa) at room temperature for 24 h. In the following, the obtained hybrid catalysts are named M-CNFOx-Rh and CX3Ox-Rh.

The actual amount of Rh loaded, determined by ICP-OES using the methodology described in the literature [26], was 0.4 wt% (39 μmol/g) in both samples. In the case of

support M-CNFOx, this percentage is calculated with respect to the mass of CNF deposited on the ceramic monolith.

Characterization

The catalysts were characterized by XPS in a VG Microtech Multilab 3000 spectrometer, and by TEM (both, fresh and used catalyst) using the same equipment as in the case of the supports.

2.3. Catalytic activity

Catalytic activity was tested in the hydrogenation of cyclohexene. Reactions were carried out in a stainless steel Parr reactor (40 mL, diameter = 2 cm), magnetically stirred, and equipped with a gas inlet valve for charging and purging the gas into the reactor and a pressure gauge for the pressure control. The experimental setup contains also a device to monitor the hydrogen consumption during the reaction.

The M-CNFOx-Rh catalyst sample used was a 7 mm long piece, with about 20 mg CNF, while about 20 mg of catalyst CX3Ox-Rh were used. The M-CNFOx-Rh catalyst piece was suspended into the reactor by means of a yarn (Figure S1) and fixed on the reactor top. In a typical experiment, the mentioned amount of catalyst and 10 mL of a 5 vol% cyclohexene in methanol solution were used. The reactor was pressurized with He and purged three times, and then H_2 was filled in and evacuated three times to finally set the H_2 pressure to 10 bar. Afterwards, the reactor was placed in the thermostatic bath at 333 K and the stirring (1100 rpm) was started. An homogeneous phase reaction was also carried out with the Rh(NN)Si complex in solution, using the proper amount of the complex dissolved in methanol and keeping all the mentioned conditions.

Previously, blank experiments without catalyst and with the support were carried out; cyclohexene conversion after 20 h was 8% and 5%, respectively. These tests indicate that in the absence of the Rh complex, the extent of the reaction is negligible compared to catalyzed systems.

Reactants and products were analyzed by gas chromatography using the HP 6890 equipment with a FID detector and a HP-1 Methyl Siloxane column (30 m-250 mm-0.25 mm).

3. Results and discussion

3.1.Characterization of supports and catalysts

Relevant data on the textural properties of the carbon materials used as support are collected in Table 1: BET surface area (S_{BET}), micropore volume (V_{μ}), mesopore volume (V_{meso}), bulk density (ρ_{bulk}), skeletal density (ρ_s) and void fraction (ε); all parameters are expressed per mass or volume of carbon. The average and maximum pore size of each material is included in Table 1.

Table 1. Textural properties of the oxidized carbon materials used as supports.

Sample	S_{BET} (m^2/g)	V_{μ} (cm^3/g)	V_{meso} (cm^3/g)	ρ_{bulk} (g/cm^3)	ρ_s (g/cm^3)	ε (-)	$w_{p,av}$ (nm)	$w_{p,max}$ (nm)
M-CNFOx	150	0.01	0.30	1.3	2.0	0.38	23	80
CX3Ox	637	0.31	1.30	0.55	2.2	0.56	20	40

The two carbon materials have very different morphology and also very different textural properties. It is interesting to notice the larger volume of mesopores of the carbon xerogel.

The layer of carbon nanofibers (CNF) has a negligible micropore volume (calculated by the t-plot method) and a significantly smaller specific surface area than the carbon xerogel support. The obtained values of surface area and pore volume are in agreement with those reported in the literature for CNF aggregates [27].

The TPD profiles of samples M-CNFOx (scrapped carbon nanofibres) and CX3Ox are shown in Figures 4a and 4b, respectively.

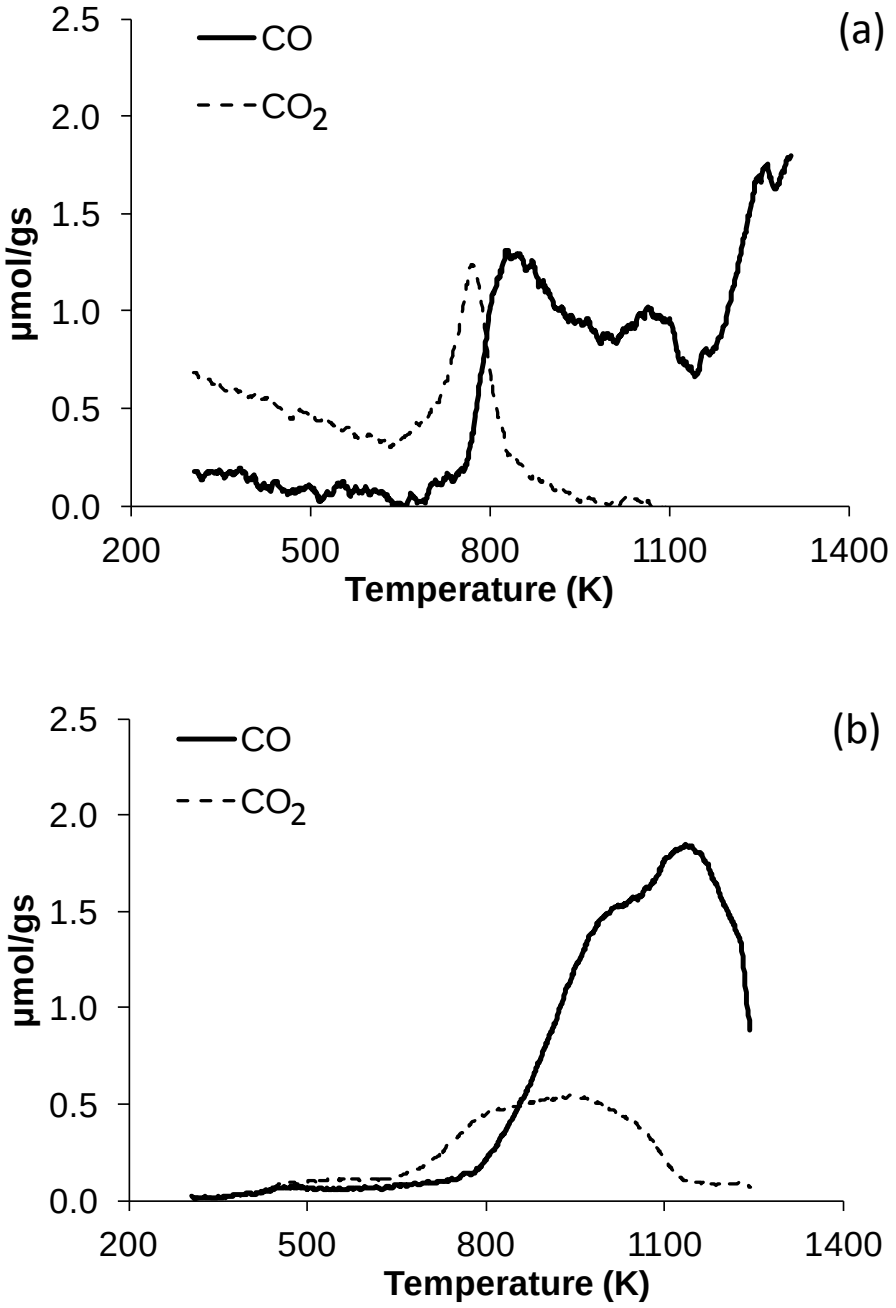

Figure 4. TPD profiles of: (a) M-CNFOx and (b) CX3Ox.

The quantification of the TPD profiles of Figure 4 is shown in Table 2. Data corresponding to the non-oxidized samples (M-CNF and CX3) are also included in Table 2 to better appreciate the effect of the oxidation treatment. The amount of phenol type groups was determined by deconvolution of the CO evolution profile in the temperature range of 873-973 K [28][29][30][31] using the Origin software.

Table 2. Quantification of TPD profiles: amounts of CO_2 and CO evolved, total oxygen (as weight percentage), and amount of phenol-type groups.

Sample	CO_2 (μmol/g)	CO (μmol/g)	O (wt. %)	Phenol-type groups [a] (μmol/g)
M-CNF	242	1868	3.8	520
M-CNFOx	457	1878	4.5	582
CX3	471	1101	3.3	314
CX3Ox	756	2021	5.7	858

[a] Determined by deconvolution of the CO desorption profile.

CO_2 evolution from sample M-CNFOx shows a maximum at about 770 K; this peak can be assigned to the decomposition of lactone and anhydride-type surface oxygen groups. The CO evolution starts at about 670 K and the profile suggests the presence of several CO-type groups, of different thermal stability, like anhydride, phenol, carbonyl and quinone [28] [29] [30][31]. The oxidation treatment with air leads to an increase of the surface oxygen complexes that decompose as CO_2, while the amount of CO-type groups remains almost unchanged.

The CO_2 evolution profile of sample CX3Ox is wider (CO_2 desorption occurs from 700 to 1100 K) and suggests the presence in this sample of surface oxygen groups like anhydride and lactone. The CO evolution starts at a relatively high temperature and shows a maximum around 1000 K, revealing the presence of a high amount of phenol and carbonyl-type groups on the sample surface. Both CO_2- and CO-type groups were generated by oxidation of the CX3Ox sample with air.

The TPD data show that the oxidation treatment is more effective in the carbon xerogel than in the grown CNF. Notwithstanding, both samples contain enough phenol-type groups to ensure a feasible anchoring of the complex (three mol of phenol-type groups per mol of Rh complex, see Figure 1).

Morphological and structural information on the supports was obtained by TEM analysis. Figure 5a shows TEM images of the carbon nanofibres of sample M-CNFOx: the CNF display a fishbone structure, with diameter ranging from 10 to 20 nm. Figure

5b shows the TEM image of sample CX3Ox, displaying a spongy appearance with a tortuous pore network.

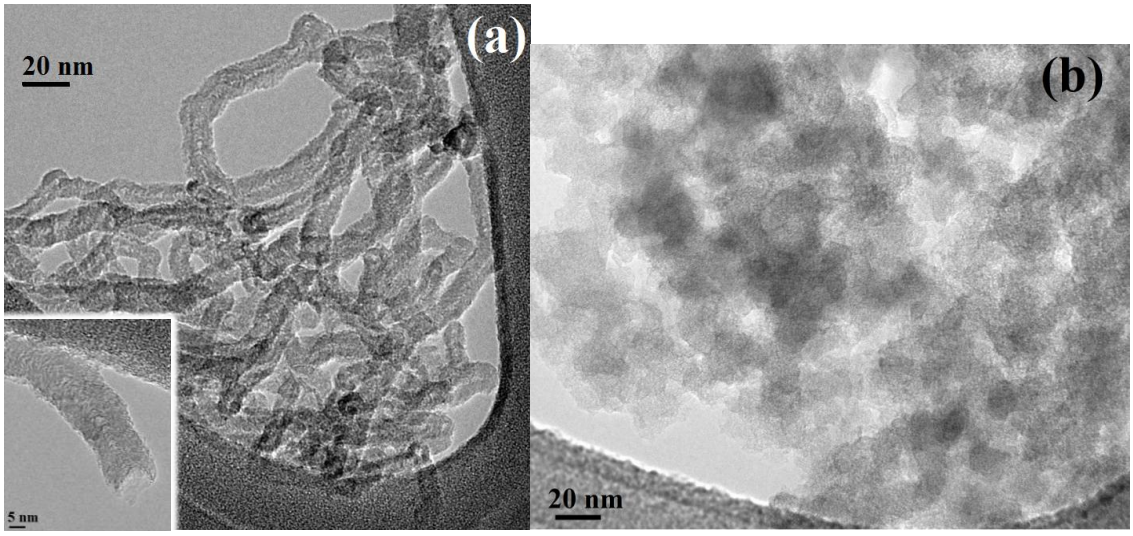

Figure 5.TEM images of (a) fibres of M-CNFOx sample and (b) CX3Ox.

The parameters determined from the XPS analysis of catalysts M-CNFOx-Rh and CX3Ox-Rh are presented in Table 3. These data show that the electronic state of Rh is almost unmodified upon heterogenization and corresponds to Rh(I). The binding energy found for N1s is characteristic of N in amine and is similar to that measured for the homogeneous complex [32].

The factor F, calculated as the ratio between the amount of Rh determined by XPS and by ICP ($F = Rh_{XPS}/Rh_{ICP}$), is close to 4 for both catalysts. This indicates that the location of the complex in relation to the support porosity is similar in both catalysts. This result is similar to that previously found with catalysts prepared with carbon nanotubes and nanofibres, where F values close to 4 were reported too [26], and lower than those reported for catalysts prepared with a microporous activated carbon (between 10 and 20) [33]. Thus, it can be considered that in the present case the Rh complex molecules are likely more internally located than in microporous activated carbon.

Table 3. XPS data of the Rh(NN)Si complex and the hybrid catalysts.

Sample	Binding energy (eV)		$F=Rh_{XPS}/Rh_{ICP}$
	$Rh3d_{5/2}$	N1s	

Rh(NN)Si	309.1	400.3	-
M-CNFOx-Rh	309.0	401.0	4
CX3Ox-Rh	308.7	400.5	4

3.2.Catalytic activity

Figure 6 shows the cyclohexene conversion versus time profiles obtained for the hybrid catalysts and the homogeneous Rh(NN)Si complex. Such conversion data have been determined from the hydrogen consumption versus time curves. TOF (s^{-1}) determined at 40 min reaction time is also shown in Figure 6 (in the legend).

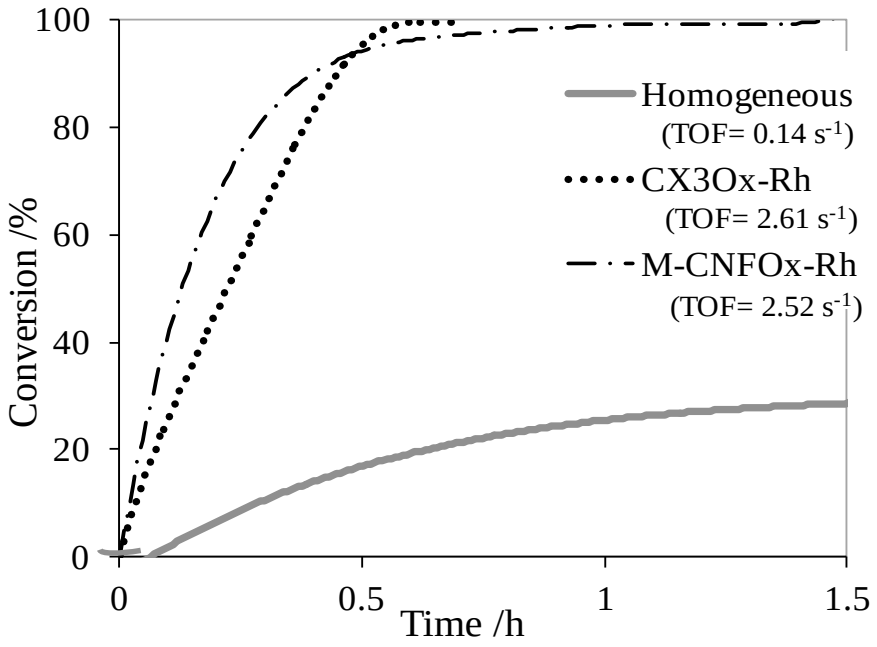

Figure 6. Cyclohexene conversion versus time of the homogeneous Rh(NN)Si complex and hybrid catalysts and TOF (at 40 min) (5 vol% cyclohexene in methanol, 10 bar H_2, 333 K, 1100 rpm).

Data of Figure 6 show that the hybrid catalysts lead to a noticeably higher conversion than the unsupported Rh complex. This was also observed with other carbon-based hybrid catalysts and it was explained by the potential confinement of the active species in the support porosity [22][26][34]. From about 1 h, both heterogeneous catalysts display similar conversion values with time, even though M-CNFOx-Rh gives a higher conversion in the first 30 min. One however notices that the conversion profile of CX3Ox seems more linear than that of M-CNFOx. The reason for this change of shape

is not clear at the moment but could come from a modification of the apparent reaction rate, due either to external/internal mass transport effects, or to a modification of the reaction pathway.

The conversion profiles of both hybrid catalysts reveal different kinetics. In the case of sample CX3Ox-Rh, the linear variation of conversion with time in the first 40 minutes suggests a 0 reaction order, probably due to diffusional problems. Such a phenomenon has been recently reported in catalysts prepared with carbon xerogels [35]. The different morphology of the two hybrid catalysts bears differences in the diffusional path length. As indicated above the CNF coating has an average thickness of 10 µm while for the 1-1.4 mm particles of CX3Ox-Rh the diffusion path is about 500-700 µm and thus diffusional limitations are very likely in this catalyst.

Thus, although the hybrid catalysts are clearly more active than the homogeneous complex, their activity could be lowered due to diffusional limitations, particularly in the case of the CX3Ox-Rh catalyst. It was attempted to check for the existence of internal diffusional limitations via the estimation of the Weisz modulus, as described in reference [35]. The Weisz modulus (Φ) is defined as the ratio between the apparent specific reaction rate and the diffusion rate of reactants in the catalyst particle. For Φ larger than 1, the internal diffusion limitations become rate-determining. The Weisz modulus is calculated by [36], at the beginning of the reaction:

$$\Phi = \frac{r_s L_p^2}{D_e \; C_s} \qquad (2)$$

where r_s is the initial apparent specific reaction rate per unit of catalyst volume (kmol m_{cat}^{-3} s^{-1}), L_p is the characteristic dimension of the catalytic media (i.e. $1/6^{th}$ of the particle diameter for spherical catalyst pellets or thickness in the case of a flat active layer), C_s is the reactant concentration at the external particle surface, and D_e is the effective diffusivity through the catalyst pores. Fast stirring of the reactor allow to assimilate it to a perfectly mixed tank so that the reactant concentration at the external particle surface C_s is close to the reactant concentration in the solution bulk at the beginning of the reaction (C_e = 0.49× 10^3 mol/L, corresponding to 5% vol. cyclohexane in methanol). The effective diffusivity is defined by:

$$D_e = \frac{\varepsilon\ D_m}{\tau} \sim \varepsilon^2 D_m \quad (3)$$

where D_m is the molecular diffusivity of the considered component (~10^{-9} m²/s for diffusion in liquids), ε is the void fraction of the catalyst and τ is tortuosity of the catalyst pores. The initial apparent specific reaction rate, r_s, is calculated from the slope of the conversion vs. time curve:

$$r_s = C_e \left(\frac{dX}{dt}\right)_{t=0} V_R \frac{\rho_{bulk}}{m_{catal}} \quad (1)$$

where $\left(\frac{dX}{dt}\right)_{t=0}$ is the slope at zero time of the tangent of the conversion curves (s^{-1}) (Fig. 6), V_R is the reactor volume (10 × 10^{-6} m^3 of reacting fluid), ρ_{bulk} is the bulk density of the catalyst (kg/m^3) which depends on the catalyst support (Table 1), and m_{catal} is the mass of catalyst used for each experiment (20 × 10^{-6} kg).

Globally, the differences between both systems are (i) the void fraction of the support (0.38 vs. 0.56 for M-CNFOx and CX3-Ox, respectively), (ii) the characteristic length of the catalyst (10 × 10^{-6} for M-CNFOx; 10^{-3}/6 m for CX3-Ox¸ assuming spherical particles) and (iii) r_s (estimated, from Fig.6, equal to about 451 and 76 kmol m_{cat}^{-3} s^{-1} for M-CNFOx-Rh and CX3-Ox-Rh, respectively). From the data gathered, Φ was found to be equal to 0.6 in the case of the monolith/CNF-supported catalyst and to 13 for the carbon xerogel-supported catalyst. In the latter case, mass transport limitations are clearly present, leading to a decrease of the catalytic activity with regard to chemical regime. In the former case, mass-transport limitations cannot be totally excluded since Φ is not much lower than 1 (please keep in mind that many values used are estimations), but these limitations are certainly less severe than in the case of the carbon xerogel. These calculations highlight the fact that, especially in liquid phase, an open texture such as that encountered in carbon xerogels does not guarantee the absence of such limitations. It is worth noticing that the pore size has no effect. In fact, the modification of the Weisz modulus between the two catalysts is mainly due to the difference in characteristic lengths, L_p.

In order to decrease mass transport effects in the case of CX3-Ox-Rh, one could envisage grinding the catalyst particles, which would lead to a decrease of L_p. However, smaller particles would be more difficult to filter and recover. So, from a technical point of view, a potential higher effectiveness is sacrificed for a better handling when particles around 1 mm are used.

Note also that, despite strong stirring, the absence of external mass transport limitations is not guaranteed, especially in the case of the xerogel-supported catalyst. Indeed, since the particles are mobile, one can consider that they are more or less immobile with the adjacent fluid, which could lead to non-negligible diffusion layer thickness. The existence of external diffusional limitations is however, in this case difficult to check; a deeper investigation, which is out of the scope of the present study, would be necessary to conclude with certainty.

After the first catalytic run (t = 1.5 h), and in order to study its reusability, the hybrid catalyst was removed from the reaction media, washed with fresh solvent and used again in a catalytic run under the same conditions. Catalyst CX3Ox-Rh was removed by filtration while catalyst M-CNFOx-Rh, due to its morphology, could be much easily extracted from the reaction media (Figure S1).

Figure 7 shows the cyclohexene conversion profiles corresponding to the first and second catalytic runs, together with the corresponding TOF at 50% conversion; TOF was calculated with the initial Rh loading.

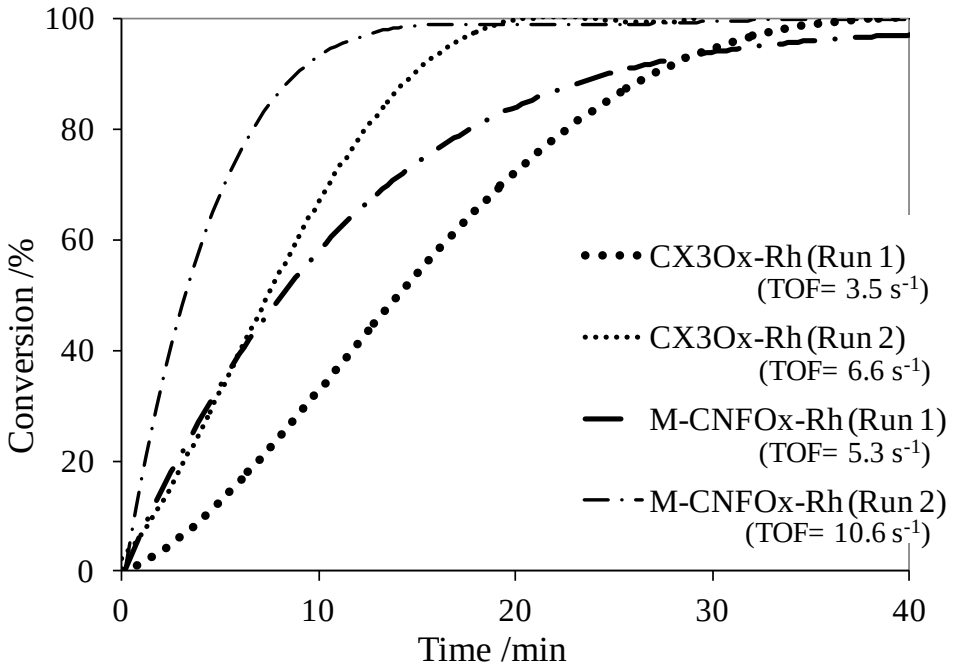

Figure 7. Cyclohexene conversion versus time and TOF (at 50% conversion), in two consecutive catalytic runs (5 vol% cyclohexene in methanol, 10 bar H_2, 333 K).

Data in Figure 7 show that both catalysts are fully recyclable with a certain increase of the catalytic activity in the second run compared with the first one. The difference in activity between catalysts is kept in the second run.

Determination of the amount of Rh in the used catalysts shows that leaching in both catalysts is low (below 4%).

The used catalysts were also analyzed by XPS and the obtained results can be summarized as follows: (i) in catalyst CX3Ox-Rh, Rh is present as Rh(I) (BE (Rh $3d_{5/2}$) = 309.9 eV) (60%) and Rh(0) (BE (Rh $3d_{5/2}$) = 307.8 eV) (40%), with no significant change of the F factor; (ii) in catalyst M-CNFOx-Rh, the Rh signals were too weak for a proper analysis; (iii) in both cases the BE of N1s is 400.9 eV, unveiling the presence of amines. These data indicate that a partial reduction of the metal complex takes place in catalyst CX3Ox-Rh, also expected in the case of M-CNFOx-Rh, and that in this last case Rh species have likely migrated to a more inner location becoming thus less accessible to the X-ray radiation.

TEM analysis of the used catalysts shows the presence of small metal particles in both of them (Figure 8), in agreement with the partial reduction of the supported metal

complex under reaction conditions shown by XPS. Size measurement of more than one hundred particles gives the data shown in Figure 9.

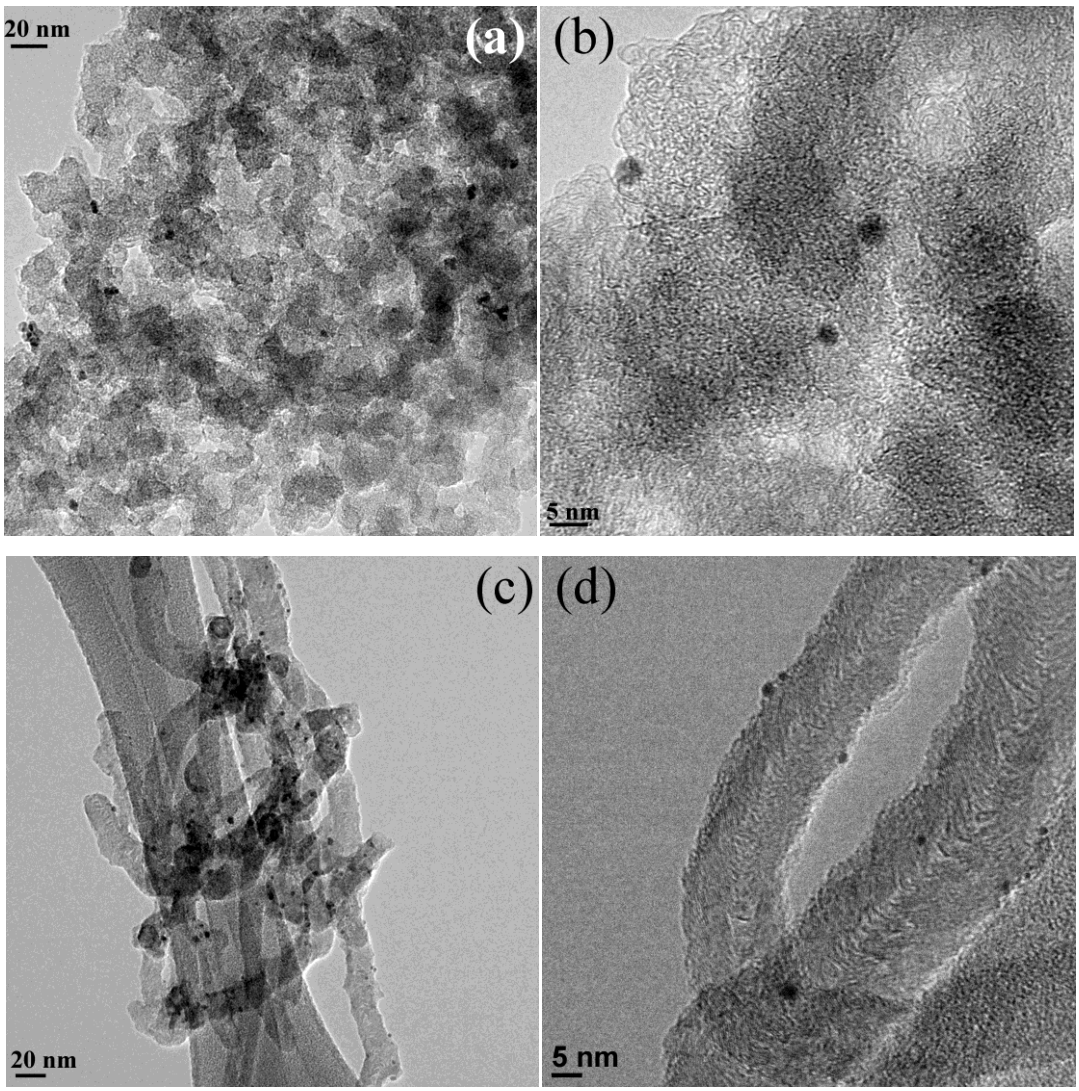

Figure 8. TEM images of used catalysts: a) and b) CX3Ox-Rh and c) and d) M-CNFOx-Rh.

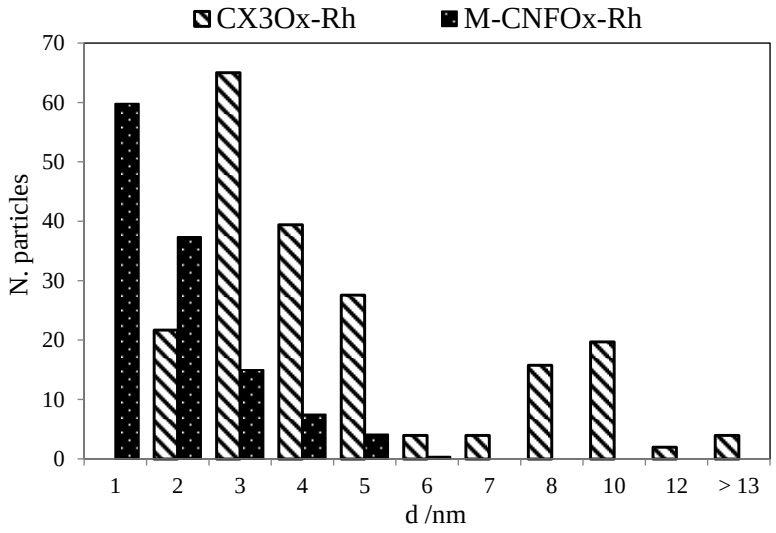

Figure 9. Particle size distribution based on a particle count of at least 100 elements.

These data show that the development of metal particles is different on both supports: they are clearly smaller in catalyst M-CNFOx-Rh. This fact can be the consequence of a different interaction of the Rh complex with the two supports. This is in agreement with previous results showing that the support has a strong influence in the properties of the hybrid catalyst [22]. In the mentioned work it was found that the surface of carbon xerogels contributes to the stabilization of the small metallic particles, whereas significant sintering takes place on some massive carbon nanofibers. In the present case, the smallest particles are developed on the carbon nanofibers, which are not massive but with a fishbone structure. However it is not possible to confirm any difference regarding the degree of reduction of the metal complex in both catalysts. According to the XPS data commented above, the active species in catalyst CX3Ox is a mixture of the supported complex Rh(NN)Si and small metallic Rh particles. In the case of catalyst M-CNFOx-Rh something similar can be assumed.

The development of small metal particles could explain the increase of the catalytic activity in the second run, although, as previously suggested, some modifications of the metal complex can also lead to more active species. The most reliable proposed modification is a change in the metal coordination sphere by hydrogenation of the cyclooctadiene ligand [33].

The obtained results show that catalysts M-CNFOx-Rh and CX3Ox-Rh are noticeably more active than the homogeneous Rh complex, stable against leaching and reusable.

They are, as well, more active than similar catalysts prepared previously with other carbon xerogels of different porous texture and with massive carbon nanofibres [22].

Moreover, catalyst M-CNFOx-Rh shows further advantages like the easy handling, the immediate recovery and removal from the reaction media avoiding the need of a filtration step, good mechanical strength and the potential to fix the catalyst to operate in continuous mode with low pressure drop.

4. Conclusions

Hybrid catalysts were prepared by anchoring covalently an Rh diamine complex in two very different structured carbon materials: a ceramic monolith coated with carbon nanofibres and a mesoporous carbon xerogel. The morphology of these catalysts allows an easy separation from the reaction media. The obtained catalysts are noticeably more active than the homogeneous Rh complex and they are stable against leaching. After a first use, a partial reduction of the Rh complex takes place and nanometric Rh particles are developed, which increases the catalyst activity. The catalyst prepared with the ceramic monolith coated with carbon fibres shows noteworthy advantages like easy handling, immediate recovery and removal from the reaction media, and good mechanical strength.

Acknowlegement: The authors thank the financial support through public projects of reference: MAT2012-32832 and PROMETEO/II/2014/010.

References

[1] E. Auer, A. Freund, J. Pietsch, and T. Tacke, “Carbons as supports for industrial precious metal catalysts,” *Appl. Catal. A Gen.*, vol. 173, no. 2, pp. 259–271, Oct. 1998.

[2] P. Serp and J. L. Figueiredo, Eds., *Carbon Materials for Catalysis*. Wiley, 2009.

[3] P. Serp, M. Corrias, and P. Kalck, “Carbon nanotubes and nanofibers in catalysis,” *Appl. Catal. A Gen.*, vol. 253, no. 2, pp. 337–358, 2003.

[4] N. Job, B. Heinrichs, S. Lambert, J.-P. Pirard, J.-F. Colomer, B. Vertruyen, and J. Marien, “Carbon xerogels as catalyst supports: Study of mass transfer,” *AIChE J.*, vol. 52, no. 8, pp. 2663–2676, Aug. 2006.

[5] N. Mager, N. Meyer, A. F. Léonard, N. Job, M. Devillers, and S. Hermans, "Functionalization of carbon xerogels for the preparation of palladium supported catalysts applied in sugar transformations," *Appl. Catal. B Environ.*, vol. 148–149, pp. 424–435, Apr. 2014.

[6] B. F. Machado, H. T. Gomes, P. Serp, P. Kalck, J. L. Figueiredo, and J. L. Faria, "Carbon xerogel supported noble metal catalysts for fine chemical applications," *Catal. Today*, vol. 149, no. 3–4, pp. 358–364, 2010.

[7] E. García-Bordejé, I. Kvande, D. Chen, and M. Rønning, "Carbon nanofibers uniformly grown on γ-alumina washcoated cordierite monoliths," *Adv. Mater.*, vol. 18, no. 12, pp. 1589–1592, 2006.

[8] N. A. Jarrah, J. G. van Ommen, and L. Lefferts, "Growing a carbon nano-fiber layer on a monolith support; effect of nickel loading and growth conditions," *J. Mater. Chem.*, vol. 14, no. 10, pp. 1590–1597, 2004.

[9] E. Armenise, S., Roldán, L., Marco, Y., Monzón, A., García-Bordejé, "Elucidation of Catalyst Support Effect for NH3 Decomposition Using Ru Nanoparticles on Nitrogen-Functionalized Carbon Nanofiber Monoliths," *J. Phys. Chem. C*, vol. 116, no. 50, pp. 26385–26395, 2012.

[10] D. R. Minett, J. P. O'Byrne, S. I. Pascu, P. K. Plucinski, R. E. Owen, M. D. Jones, and D. Mattia, "Fe@CNT-monoliths for the conversion of carbon dioxide to hydrocarbons: structural characterisation and Fischer-Tropsch reactivity investigations," *Catal. Sci. Technol.*, vol. 4, no. 9, pp. 3351–3358, 2014.

[11] S. Morales-Torres, A. F. Pérez-Cadenas, F. Kapteijn, F. Carrasco-Marín, F. J. Maldonado-Hódar, and J. A. Moulijn, "Palladium and platinum catalysts supported on carbon nanofiber coated monoliths for low-temperature combustion of BTX," *Appl. Catal. B Environ.*, vol. 89, no. 3–4, pp. 411–419, Jul. 2009.

[12] J. Zhu, Y. Jia, M. Li, M. Lu, and J. Zhu, "Carbon Nanofibers Grown on Anatase Washcoated Cordierite Monolith and Its Supported Palladium Catalyst for Cinnamaldehyde Hydrogenation," *Ind. Eng. Chem. Res.*, vol. 52, no. 3, pp. 1224–1233, Jan. 2013.

[13] K. M. De Lathouder, J. J. W. Bakker, M. T. Kreutzer, S. A. Wallin, F. Kapteijn, and J. A. Moulijn, "Structured Reactors for Enzyme Immobilization: A Monolithic Stirrer Reactor for Application in Organic Media," *Chem. Eng. Res. Des.*, vol. 84, no. 5, pp. 390–398, May 2006.

[14] Y. Marco, E. García-Bordejé, C. Franch, A. E. Palomares, T. Yuranova, and L. Kiwi-Minsker, "Bromate catalytic reduction in continuous mode using metal catalysts supported on monoliths coated with carbon nanofibers," *Chem. Eng. J.*, vol. 230, pp. 605–611, Aug. 2013.

[15] T. Yuranova, L. Kiwi-Minsker, C. Franch, A. E. Palomares, S. Armenise, and E. García-Bordejé, "Nanostructured Catalysts for the Continuous Reduction of Nitrates and Bromates in Water," *Ind. Eng. Chem. Res.*, vol. 52, no. 39, pp. 13930–13937, Oct. 2013.

[16] J. Restivo, J. J. M. Órfão, M. F. R. Pereira, E. Garcia-Bordejé, P. Roche, D. Bourdin, B. Houssais, M. Coste, and S. Derrouiche, "Catalytic ozonation of organic micropollutants

using carbon nanofibers supported on monoliths," *Chem. Eng. J.*, vol. 230, pp. 115–123, Aug. 2013.

[17] N. Job, R. Pirard, J. Marien, and J. P. Pirard, "Porous carbon xerogels with texture tailored by pH control during sol-gel process," *Carbon N. Y.*, vol. 42, no. 3, pp. 619–628, 2004.

[18] N. Job, A. Théry, R. Pirard, J. Marien, L. Kocon, J.-N. Rouzaud, F. Béguin, and J.-P. Pirard, "Carbon aerogels, cryogels and xerogels: Influence of the drying method on the textural properties of porous carbon materials," *Carbon N. Y.*, vol. 43, no. 12, pp. 2481–2494, Oct. 2005.

[19] F. Maia, N. Mahata, B. Jarrais, A. R. Silva, M. F. R. Pereira, C. Freire, and J. L. Figueiredo, "Jacobsen catalyst anchored onto modified carbon xerogel as enantioselective heterogeneous catalyst for alkene epoxidation," *J. Mol. Catal. A Chem.*, vol. 305, no. 1–2, pp. 135–141, 2009.

[20] E. Bailón-García, F. Carrasco-Marín, A. F. Pérez-Cadenas, and F. J. Maldonado-Hódar, "Development of carbon xerogels as alternative Pt-supports for the selective hydrogenation of citral," *Catal. Commun.*, vol. 58, pp. 64–69, Jan. 2015.

[21] N. Job, J. Marie, S. Lambert, S. Berthon-Fabry, and P. Achard, "Carbon xerogels as catalyst supports for PEM fuel cell cathode," *Energy Convers. Manag.*, vol. 49, pp. 2461–2470, 2008.

[22] C. C. Gheorghiu, C. SalinasMartínezdeLecea, and M. C. RománMartínez, "Support effects in a Rh diamine complex heterogenized on carbon materials," *ChemCatChem*, vol. 5, no. 6, pp. 1587–1597, 2013.

[23] E. García-Bordejé, I. Kvande, D. Chen, and M. Rønning, "Synthesis of composite materials of carbon nanofibres and ceramic monoliths with uniform and tuneable nanofibre layer thickness," *Carbon N. Y.*, vol. 45, no. 9, pp. 1828–1838, 2007.

[24] S. Armenise, M. Nebra, E. García-Bordejé, and A. Monzón, *Scientific Bases for the Preparation of Heterogeneous Catalysts - Proceedings of the 10th International Symposium, Louvain-la-Neuve, Belgium, July 11-15, 2010*, vol. 175. Elsevier, 2010.

[25] F. Rodríguez-Reinoso and A. Linares-Solano, *Chemsitry and Physics of Carbon, Vol 21*. New York: Dekker, 1988.

[26] L. J. Lemus-Yegres, M. C. Román-Martínez, I. Such-Basáñez, and C. Salinas-Martínez de Lecea, "Effects of confinement in hybrid diamine-Rh complex-carbon catalysts used for hydrogenation reactions," *Microporous Mesoporous Mater.*, vol. 109, no. 1–3, pp. 305–316, 2008.

[27] K. P. de Jong and J. W. Geus, "Carbon Nanofibers: Catalytic Synthesis and Applications," *Catal. Rev.*, vol. 42, no. 4, pp. 481–510, Feb. 2000.

[28] J. . Figueiredo, M. F. . Pereira, M. M. . Freitas, and J. J. . Órfão, "Modification of the surface chemistry of activated carbons," *Carbon N. Y.*, vol. 37, no. 9, pp. 1379–1389, Jan. 1999.

[29] S. Haydar, C. Moreno-Castilla, M. A. Ferro-García, F. Carrasco-Marín, J. Rivera-Utrilla, A. Perrard, and J. P. Joly, "Regularities in the temperature-programmed desorption spectra of CO2 and CO from activated carbons," *Carbon N. Y.*, vol. 38, no. 9, pp. 1297–1308, Jan. 2000.

[30] G. S. Szymański, Z. Karpiński, S. Biniak, and A. Świątkowski, "The effect of the gradual thermal decomposition of surface oxygen species on the chemical and catalytic properties of oxidized activated carbon," *Carbon N. Y.*, vol. 40, no. 14, pp. 2627–2639, Jan. 2002.

[31] J. H. Zhou, Z. J. Sui, J. Zhu, P. Li, D. Chen, Y. C. Dai, and W. K. Yuan, "Characterization of surface oxygen complexes on carbon nanofibers by TPD, XPS and FT-IR," *Carbon N. Y.*, vol. 45, no. 4, pp. 785–796, 2007.

[32] "lasurface." [Online]. Available: http://www.lasurface.com/accueil/index.php.

[33] L. J. Lemus-Yegres, I. Such-Basáñez, M. C. Román-Martínez, and C. S. M. de Lecea, "Catalytic properties of a Rh-diamine complex anchored on activated carbon: Effect of different surface oxygen groups," *Appl. Catal. A Gen.*, vol. 331, no. 1, pp. 26–33, 2007.

[34] S. Pariente, P. Trens, F. Fajula, F. Di Renzo, and N. Tanchoux, "Heterogeneous catalysis and confinement effects," *Appl. Catal. A Gen.*, vol. 307, no. 1, pp. 51–57, Jun. 2006.

[35] S. L. Pirard, C. Diverchy, S. Hermans, M. Devillers, J.-P. Pirard, and N. Job, "Kinetics and diffusional limitations in nanostructured heterogeneous catalyst with controlled pore texture," *Catal. Commun.*, vol. 12, no. 6, pp. 441–445, Feb. 2011.

[36] G. F. Froment, K. B. Bischoff, and J. De Vilde, *Chemical Reactor Analysis and Design*, 3rd ed. John Wiley and Sons, 2011.

Supporting information

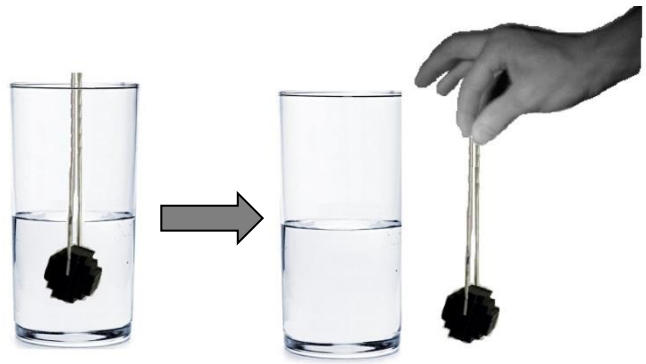

Figure S1. Location in the reactor and removal from it, of catalyst M-CNFOx-Rh.